Silica microspheres array strain sensor

Marta S. Ferreira,[1,2,*] José L. Santos,[1,2] and Orlando Frazão[1,2]

[1]*INESC Porto, Rua do Campo Alegre 687, Porto 4169-007, Portugal*

[2]*Departamento de Física da Faculdade de Ciências da Universidade do Porto, Rua do Campo Alegre 687, Porto 4169-007, Portugal*

**Corresponding author: msaf@inesctec.pt*

Received July 25, 2014; revised September 13, 2014; accepted September 16, 2014;
posted September 16, 2014 (Doc. ID 217768); published October 10, 2014

An optical fiber sensor based on arrays of silica microspheres is proposed. The microspheres are produced separately using a fusion splicer and then also connected in series by fusion splicing. Three different sensors are presented, differing by the number of microspheres. Due to the geometry of the structures, different behaviors are obtained in strain measurements. Sensors with an odd number of microspheres are more sensitive to strain than the ones with an even number of microspheres. Additionally, the sensing heads are subjected to temperature where a sensitivity of 20.3 pm/°C is obtained in a range of 200°C.

OCIS codes: (060.2370) Fiber optics sensors; (120.3180) Interferometry.
http://dx.doi.org/10.1364/OL.39.005937

In 1995, the first paper on the excitation of a microsphere with external beams was published [1]. The polystyrene microsphere was placed on an optical-fiber coupler and the resonances were measured in an aqueous environment. Different approaches have been proposed to couple light into microspheres. For instance, the use of a prism, produced by the angle polishing of the end face of a fiber [2], or the use of tapers [3] have been studied. All of these configurations take advantage of the whispering gallery modes that are achieved due to the structure spherical geometry. This feature translates into optical resonators with high-quality factors [4] that can be applied both passively and actively. In the first case, the microsphere resonators can be used as optical sensors. These structures have been proposed for several applications, such as biosensing [5], temperature sensing [6], and radiation pressure [7], among others. Additionally, when the microspheres are doped with rare-earth elements, these resonators can be used as microlasers, where large free-spectral range and single-mode operation are easily achievable [4]. There are two different ways to produce silica microspheres at the end of a fiber section: through CO_2 laser [3,8] or electric-arc discharges produced by a splice machine [5].

Two different mechanisms have been established to explain the propagation of light in an array of microspheres. The first is due to the tight binding of the whispering gallery modes. The second mechanism is related to the focusing produced by the cavities. This binding translates in a propagation of periodic modes along the microspheres, designated as "nanojet induced modes" [9]. These mechanisms have been theoretically and experimentally demonstrated using polystyrene [10] and sapphire [11] microspheres ordered in arrays. In these works, the first microsphere of the array was fully illuminated by the optical source, and the microspheres had both dimensions and refractive indices that enabled the focusing of light at the shadow surface of the spheres [10,11].

In this Letter, a different approach is presented using microspheres produced in standard single-mode fiber. Several sensing heads are produced by splicing microspheres in series to produce an array. In this case, the light propagation occurs inside the whole structure. The sensing structures are tested to strain and temperature.

Figure 1 presents the growth of a microsphere (μsphere) at the end face of a standard single-mode fiber (SMF28) section. The microspheres were produced using the Fitel S182PM splice machine, in the polarization-maintaining (PM) manual program. The arc power was 110 a.u., the prefuse time was 240 ms, and the arc duration was 2000 ms. The fiber was cleaved and inserted in the splice machine. Afterward, it was moved forward ~125 μm ensuring that the arc discharge occurred in the SMF28 region. In the first photograph of Fig. 1 the two arrows represent the position of the electrodes relative to the fiber.

From the second photo on, each picture in Fig. 1 was taken under the microscope after applying a one-arc discharge. The high power of the electric discharge was transferred to the fiber tip, which partially melted. Due to the surface tensions, the fiber acquired the spherical shape observed in Fig. 1.

The microsphere diameter was measured after each electric-arc discharge and depicted in the graph of Fig. 2. There is stronger growth at the beginning of the

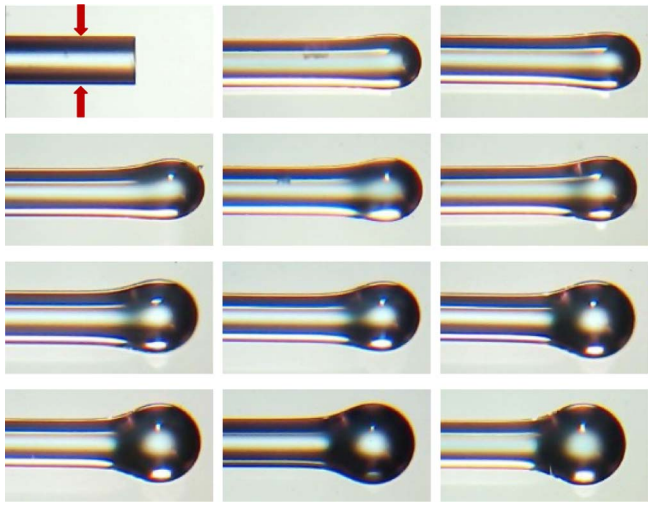

Fig. 1. Microspheres manufacturing process, using the splice machine. Each photo was taken after one electric arc.

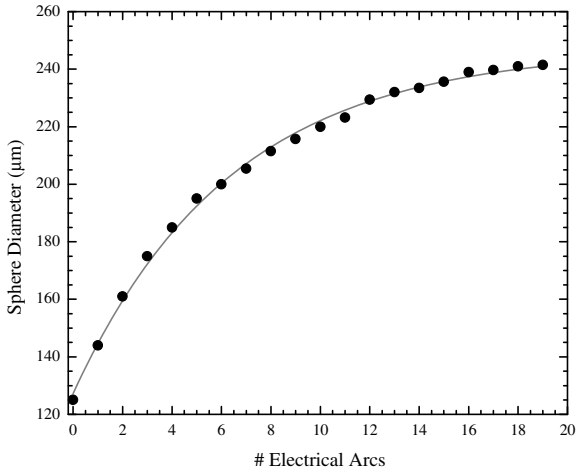

Fig. 2. Dependence of the sphere diameter with the number of electric arcs.

fabrication (first seven arc discharges). After that point, the diameter increase is less pronounced, as can be seen in Fig. 2. With this method, after a certain amount of electric discharges the microsphere growth tends to stabilize. A final diameter of ~240 μm was attained, after 18 electric arc discharges. The mean diameter of the microspheres used in this work was 228.5 μm.

Three different structures were produced by connecting 2, 3, and 4 μspheres in series. The microscope photos of each sensor are shown in Fig. 3. The 2-μspheres [Fig. 3(a)] sensor was fabricated by fusion splicing 2 μspheres that were produced separately. This fusion was done using the same program of the splice machine, with the 2 μspheres aligned, and a total of five electric arcs were applied to ensure the mechanical stability of the sensor without collapsing the microspheres. The 3-μspheres sensor shown in Fig. 3(b) was produced as follows. First, the microspheres were all fabricated separately. Afterward, 2 μspheres were fusion spliced as previously described. A cleave was then made after the second microsphere, which was spliced to the third one. Regarding the 4-μspheres sensor [see Fig. 3(c)], the manufacturing process was the same as the previous one.

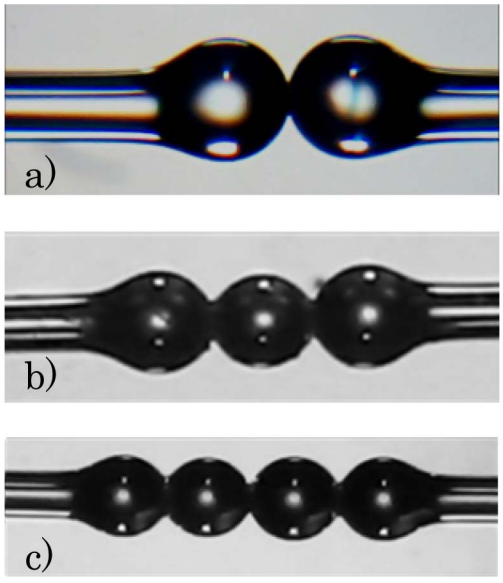

Fig. 3. Scheme of the experimental setup. The photo of the sensing heads with (a) 2 μspheres, (b) 3 μspheres, and (c) 4 μspheres are also shown.

The sensing head was connected between a broadband optical source and an optical spectrum analyzer (OSA). The optical source had a bandwidth of 100 nm and was centered at 1570 nm. Transmission readings were done with a resolution of 0.2 nm.

The optical-path difference of light traveling in the microspheres gives rise to interferometric behavior, and to understand its basic characteristics the light propagation in the microspheres was simulated using the Zemax SE optical-design software.

The microspheres were simulated as ball lenses of fused silica, with a refractive index of 1.44402 at 1550 nm. It was also considered that the object numerical aperture was the same as SMF28, translating in the divergence of the beam observed in Fig. 4. The simulations were performed as a first approach and did not take the polarization of light into account. Due to the broadening of the fiber in the region close to the first microsphere, the light seems to exit near a punctual source (core of the SMF fiber) located before the microsphere (point f_1 in Fig. 4). As light passes through the first microsphere, the beam will diverge, whereas in the second microsphere, there will be a convergence of the beam. For the case of the 2-μspheres sensor, light will be recoupled in the SMF28 region. Thus, the interference pattern observed in the spectrum of the top of Fig. 5 occurs due to the optical-path difference of light that travels from point f_1, associated with the first microsphere, to the exit fiber core connected with the second microsphere. Therefore, as illustrated in Fig. 4(a), a Mach–Zehnder type interferometric pattern is expected, which is confirmed by the clear two-wave channeled spectrum behavior shown at the top of Fig. 5.

With the addition of a third microsphere the light will converge inside it, at the point indicated as f_2 in Figs. 4(b) and 4(c). Notice that in Fig. 4(b) there is further

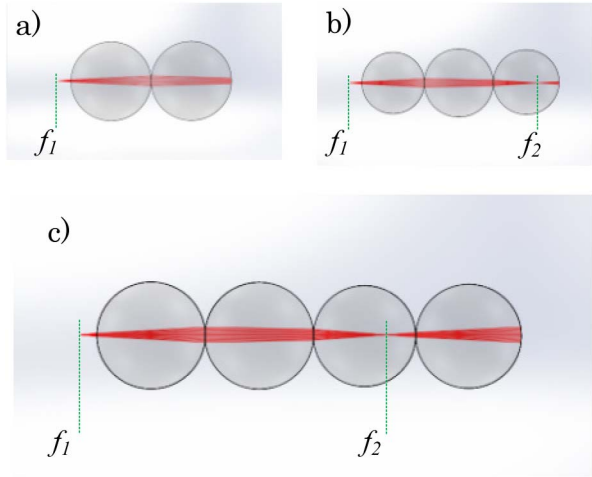

Fig. 4. Microspheres array sensors modeling using Zemax, considering (a) 2-μspheres, (b) 3-μspheres and (c) 4-μspheres. Also shown the focal points f_1 and f_2 for each configuration (when applicable).

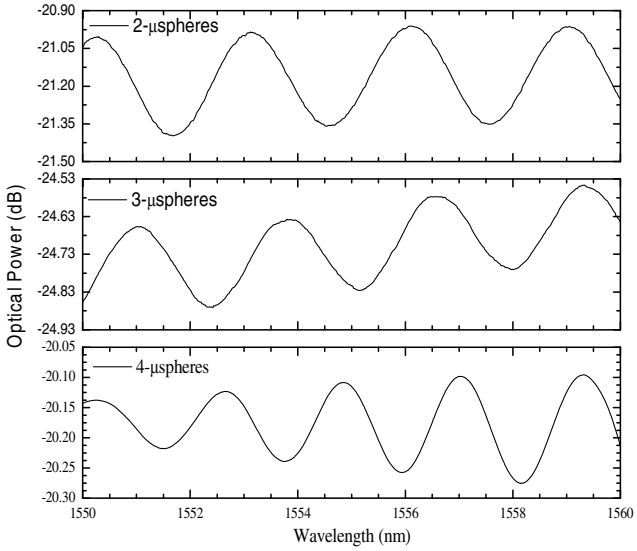

Fig. 5. Channeled spectra of light that exits the sensing heads with 2 (top), 3 (middle), and 4 (bottom) μspheres.

divergence of the beam after f_2. Nevertheless, it will not have much influence on the power coupling to the output SMF28 since it is very close to the edge of the microsphere. However, when a fourth microsphere is introduced, the beam will broaden once more, originating some change on the amount of optical power that propagates down the exit fiber (the vertical scale in Fig. 4 does not follow these trends exactly due to different insertion losses derived from the addition of another microsphere). The two points, f_1 and f_2, are associated with light focusing and therefore can be identified as focal points. Maximum transmission through the microsphere system occurs when the location of the last focal point happens close to the exit surface of the last microsphere.

When further microspheres are integrated into the chain, there are more possibilities for different propagation lengths from the input SMF28 to the output one. Therefore, additional waves are generated with non-negligible amplitude that add together with the two main waves, generating an interference pattern with an envelope modulation compared with the base two-wave interferogram, which becomes more pronounced when the number of these additional waves increases as a consequence of cascading an increasing number of microspheres. The observation of Fig. 5 (middle and bottom) indicates the validity of this argument.

Strain measurements were done by placing the sensors in a translation stage with a resolution of 0.01 mm. Figure 6 shows the experimental results of the multiple sensing heads when subjected to strain, while the strain sensitivities are presented in Table 1. A dependence on the number of microspheres is clear. These results and the ray-trace analysis performed seem to indicate the sensitivity is a function based on the number of microspheres that are even or odd and associated with the fact that for an odd number there will be a focal point near the input of the output SMF 28 [as happens for the case of 3-μspheres shown in Fig. 4(b)].

The sensing heads were subjected to temperature variations. In order to do that, they were placed in a tubular

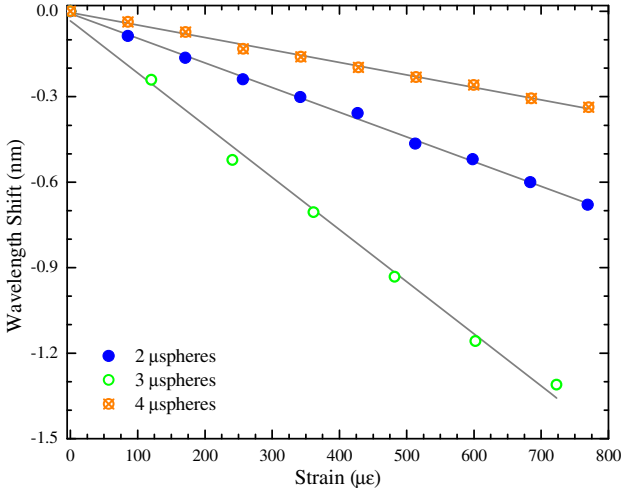

Fig. 6. Sensing heads' response to the applied strain.

Table 1. Strain Sensitivity Obtained for Each Sensor

No. of Microspheres	Sensitivity (pm/με)
2	−0.87
3	**−1.59**
4	−0.44

oven, and measurements were done in a range of 200°C, with a resolution of 0.1°C. Linear behavior was observed and the sensitivity attained was the same for the three sensors, which was ~20 pm/°C. The positive behavior results from the thermal expansion of the silica microspheres.

In summary, the use of an array of microspheres can provide sensing structures with characteristics that can be tailored to specific applications. In this work, different sensing heads were manufactured, with the number of microspheres connected in series ranging from 2 to 4. The sensing heads were subjected to strain and temperature. The 3-μspheres sensor was the most sensitive to strain, with twice the sensitivity obtained for the 2-μspheres sensor and four times the value attained for the 4-μspheres sensor. The sensitivity to temperature was found to be independent of the number of microspheres in the structure.

This work was supported by FCT—Fundação para a Ciência e Tecnologia (Portuguese Foundation for Science and Technology) under the grant SFRH/BD/76965/2011. It was also financed by the ERDF (European Regional Development Fund) through the COMPETE Programme (operational programme for competitiveness) and by National Funds through the FCT within Project FCOMP-01-0124-FEDER-037281.

References

1. A. Serpengüzel, S. Arnold, and G. Griffel, Opt. Lett. **20**, 654 (1995).
2. N. M. Hanumegowda, C. J. Stica, B. C. Patel, I. White, and X. Fan, Appl. Phys. Lett. **87**, 201107 (2005).
3. K. J. Vahala, Nature **424**, 839 (2003).
4. J. Ward and O. Benson, Laser Photon. Rev. **5**, 553 (2011).
5. S. Soria, S. Berneschi, M. Brenci, F. Cosi, G. N. Conti, S. Pelli, and G. C. Righini, Sensors **11**, 785 (2011).

6. J. M. Ward and S. N. Chormaic, Appl. Phys. B **100**, 847 (2010).
7. R. Ma, A. Schliesser, P. Del'Haye, A. Dabirian, G. Anetsberger, and T. J. Kippenberg, Opt. Lett. **32**, 2200 (2007).
8. M. Sumetsky, Y. Dulashko, and R. S. Windeler, Opt. Lett. **35**, 898 (2010).
9. Z. Chen, A. Taflove, and V. Backman, Opt. Lett. **31**, 389 (2006).
10. S. Yang and V. N. Astratov, Appl. Phys. Lett. **92**, 261111 (2008).
11. A. Darafsheh and V. N. Astratov, Appl. Phys. Lett. **100**, 061123 (2012).